Flaring Rate of Northern Blazars

Lauren Hindman

A senior thesis submitted to the faculty of
Brigham Young University
in partial fulfillment of the requirements for the degree of

Bachelor of Science

J. Ward Moody, Advisor

Department of Physics and Astronomy

Brigham Young University

ABSTRACT

Flaring Rate of Northern Blazars

Lauren Hindman
Department of Physics and Astronomy, BYU
Bachelor of Science

Blazars, a subclass of Active Galactic Nuclei (AGN), are characterized by a jet of particles accelerated by magnetic fields around supermassive black holes. For blazars, these jets are angled toward Earth. These objects are known to change magnitude, or flare, often and sometimes rapidly. It is thought that two mechalisms are mainly responsible for flaring: geometric instabilities in the jets which occur stochastically, and periodic changes in jet or accretion disk activity add oriendation from orbital perturbations. Using our Remote Observatory for Variable Object Research (ROVOR), we monitored 192 of these objects using both V and R Johnson broadband spectral filters over the course of a year. We comment on the variability observed and which mechanism may be most responsible.

Keywords: Quasar, Active Galactic Nuclei

Contents

Table of Contents iii

1 Introduction 1
- 1.1 Blazars; What We Know 1
- 1.2 Ongoing Work 2
- 1.3 Purpose 3
- 1.4 Organization 3

2 Method 4
- 2.1 Object Selection 4
- 2.2 Observations and Reduction 4
- 2.3 Statistical Approach 6

3 Results 7
- 3.1 Data 7
- 3.2 Conclusions 20

Chapter 1

Introduction

1.1 Blazars; What We Know

A class of active galactic nuclei (AGN) called quasars are believed to be among the most luminous and energetic objects in the universe. Quasars are relativistic jets thought to form when charged matter in accretion disks around supermassive black holes (SMBH) interacts with their helical magnetic field. When these jets are pointing toward Earth they are considered blazars.

Blazars are known to vary in brightness, or flare, regularly as well as rapidly. Flares occur at seemingly random intervals and can occur on short timescales (<1 hour) as well as long (>6 months) (Smith, Nair 1994). Some even vary at multiple timescales simultaneously.

Blazars are a not well understood subclass of AGN, especially when it comes to what causes these flares. To be clear, there are a few blazars whose physical attributes we understand quite well, but this is only the case after many years of constant observation. The flaring mechanisms found in these particular objects typically seem to be unique to that particular blazar.

Over the past decade, a few theories for general flaring mechanisms have been determined. Smooth, regular flares are attributed to orbital motion of the black hole itself, or environmental

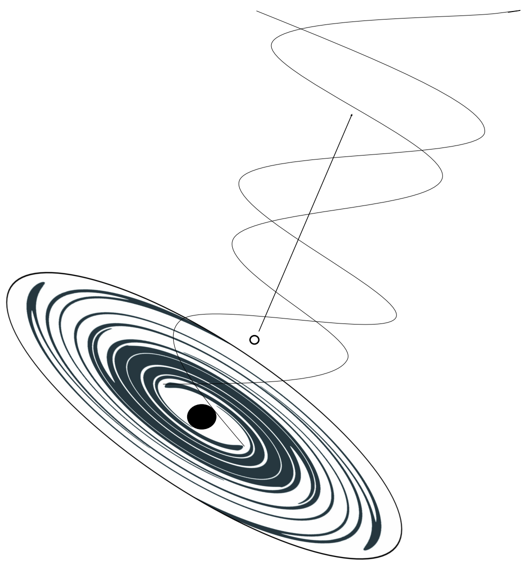

Figure 1.1 matter being accelerated away from a SMBH.

factors such as the possibility of a binary black hole system. Erratic flaring is thought to be caused by instabilities in the jet. It is possible both of these mechanisms are at play in most blazars. Dominant mechanisms in each blazar should be reflected in behaviour.

1.2 Ongoing Work

Particularly bright blazars are monitored for flaring across the world by an organization called the Whole Earth Blazar Telescope (WEBT), though they tend to focus on the more famous blazars. While a few of these objects are regularly observed, many others that are easily bright enough to be observed optically with small ground based telescopes are typically disregarded for long term study. Many have not even been observed since their discovery!

1.3 Purpose

By observing a large sample of these objects we are hoping to find the flaring rate for a general population. We also are attempting to determine what blazars are currently exhibiting flaring behaviour which are not part of the famous population, and calculate current baseline magnitudes. By finding a greater population of interesting blazars, we can gain the interest of larger organizations such as WEBT and get some further analysis underway.

Widening our view and understanding of this phenomena will help us better understand the environment surrounding these black holes and the processes they go through.

Additionally, we hope the quality of our findings will encourage other researchers with access to smaller telescopes such as ours to be able to research optical variability, opening the door to a population of researchers previously rarely involved in this kind of research.

1.4 Organization

This paper is organized as follows. Section two describes our observational methods, calibrations, and approach to analyzing data. In section three we discuss our results.

Chapter 2

Method

To observe flares and calculate updated magnitudes, data were gathered from June 2015 to June 2016 using BYU's 16" ROVOR telescope (Moody *et al.* 2012). Photometry was performed using the software MIRA.

2.1 Object Selection

Candidate objects were chosen from the following astronomical catalogs: American Ephemeris, Veron Cetty-Veron (Veron Cetty-Veron 2010) AGN catalog, and the Whole Earth Blazar Telescope (WEBT) list of high-energy blazars. Objects were included based on the following criteria: optical magnitudes brighter than 16.0, declination above 0°.

2.2 Observations and Reduction

Objects were observed between 3 to 22 nights throughout the year using ROVOR. Each observation consisted of six one-minute images in the Johnson V filter and five one-minute images in Johnson R.

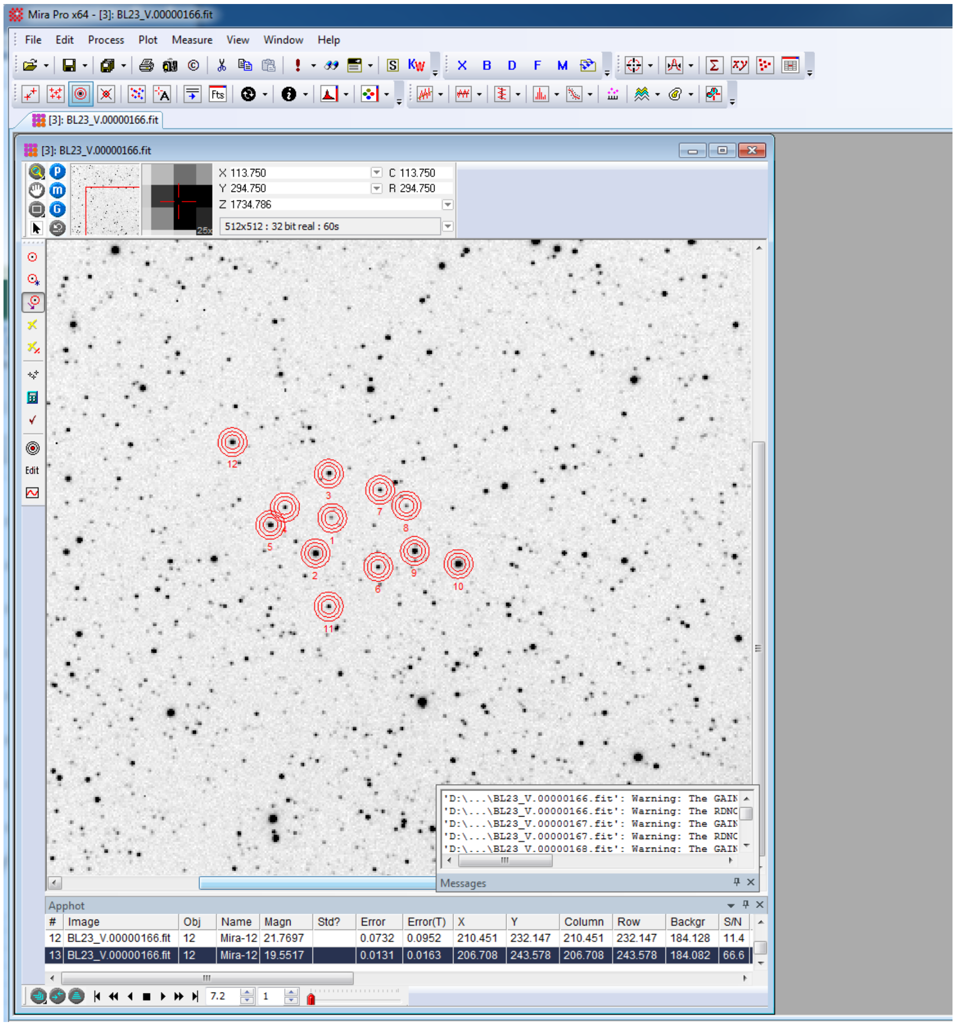

Figure 2.1 Photometry in MIRA with 11 standard objects. Circles represent each aperture. The blazar is listed as object one. The standards are the following 11 objects

Photometry, or extracting photon flux data from images, was performed using MIRA. With few exceptions, the aperture size was consistently 4, 6, and 8 pixels; one pixel is equivalent to 2.7 arcseconds. Figure 2.1 shows the overlay of the aperture the object. The ring outside of the aperture helps with reducing error by integrating the background light in the field and subtracting it from the aperture data. As you can see in figure 2.1, additional objects had photometry performed on them to decrease our statistical error. These 11 objects are assumed to be standard.

An unexpected and irritating source of error arising in recent years when using ROVOR is what we call a herringbone pattern. Such patterns arise from a periodic ground plane voltage fluctuation in our power source. Recently we have found increasing the annulus size in MIRA significantly reduces the error from this fluctuation.

2.3 Statistical Approach

Flat fields, Darks and Biases, following standard photometry practices, were applied to each frame before magnitudes were gathered. To increase reliability of photometry, 11 standard objects were chosen within each field. These stars were compared with each other and only those with sufficient signal and stability were used to calibrate the blazar.

The trend in magnitude vs time for each object was fit to a third degree polynomial. The R^2 coefficient given in each fit gives the correlation coefficient.

To determine reliability of our data, the standard deviation of the data with respect to the fit was, in each filter, compared to the standard deviation of the difference between filters. A ratio greater than two in both filters means the filters were tracking together over time as would be expected for low observational noise. Therefore this ratio was used as an indicator that error from the atmosphere is neglegable.

Chapter 3

Results

3.1 Data

Magnitudes averaged over our observations can be seen in table 3.1. In the table, the R^2 value indicates the fit of a second degree polynomial to the data. As we interpret it, a value < 0.35 indicates stochastic variance and a value >0.75 indicates smooth variance.

Figure 3.1 shows the normalized magnitudes of the blazars over time. By normalized we mean that he first magnitude in the sequence for each object was set to be the same value of 0.0. Subsequent points show how much the magnitude varied from the first value. Thirteen objects stood out with significant change in magnitude and a standard deviation ratio greater than two in both V and R filters. Those objects are outlined in the top right corner. Three of those are in the famous population, but the others are being identified as highly variable for the first time in this study. The rest of the 192 objects are graphed behind the 13 in yellow to indicate that their variability was not significant.

We have successfully found current baseline values for these 192 objects. These baselines can be viewed in table 3.1 along with their correlation coefficients. Data missing in the table indicates

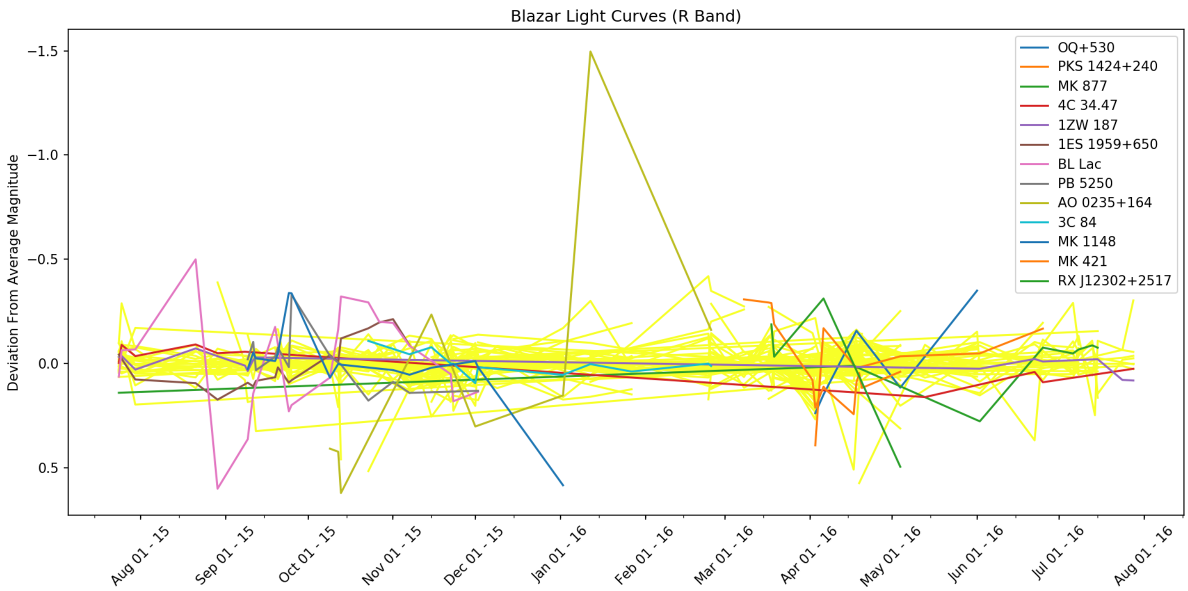

Figure 3.1 Normalized reduced data. Note Magnitude scale is inverted; smaller magnitudes indicate brighter object.

objects we were unsuccessful in observing often enough to be statistically significant.

Number	Object	R.A.	Dec	VC MAG	Measured V	Measured R	R^2
1	4C 25.01	0 19 39.8	+26 2 52	15.4	16.05	15.75	0.73
2	A 0021+25	0 24 9.4	+5 25 8	15.1	15.715	15.04	0.24
3	PG 0026+129	0 29 13.8	+13 16 5	15.4	15.44	15.14	0.76
4	PB 6151	0 45 47.2	+ 4 10 24	16	16.19	15.82	0.25
5	MK 1148	0 51 54.8	+17 25 59	16	15.517	15.13	0.33
6	1ZW 1	0 53 34.9	+12 41 36	14	14.16	13.71	0.65
7	PG 0052+251	0 54 52.2	+25 25 39	15.4	15.31	15.09	0.36
8	PHL 909	0 57 9.9	+14 46 11	15.7	16.24	15.86	0.090
9	IRAS 01072-0348	1 9 45.1	-3 32 33	13	15.79	15.47	0.62
10	GC 0106+224	1 9 45.1	+22 44 39	15.7	15.14	14.69	0.49
11	MK 375	1 22 40.6	+23 10 15	15.4	15.34	15.16	0.19
12	1ES 0120+340	1 23 8.7	+34 20 49	15.2	17.7	16.61	0.75
13	IRAS 01475+3554	1 50 32.7	+36 9 26	15.3	16.50	15.96	0.79
14	S5 0153+74	1 57 34.8	+74 42 44	16	17.05	16.43	0.43
15	MK 1014	1 59 50.2	+0 23 41	15.7	15.74	15.40	0.80
16	MK 586	2 7 49.8	+2 42 55	15.4	15.60	15.39	0.21
17	3C 59	2 7 2.2	+29 30 45	16	16.79	16.24	0.55
18	PKS 0215+015	2 17 48.9	+1 44 50	15.4	18.30	19.32	1

Number	Object	R.A.	Dec	VC MAG	Measured V	Measured R	R^2
19	B3 0225+389	2 28 59.2	+39 8 45	15.8	18.83	17.86	0.11
20	1ES 0229+200	2 32 48.6	+20 17 17	14.7	16.88	16.14	0.14
21	AO 0235+164	2 38 38.9	+16 37 0	15.5	18.41	17.50	0.24
22	S2 0241+62	2 44 57.6	+62 28 6	15.7	16.75	15.66	0.68
23	4U 0241+61	2 45 19.1	62 29 14	12.2	16.86	15.69	0.31
24	3C 48	3 19 48.16	+41 30 42.1	12.5	13.12	12.52	0.82
25	3C 110	4 17 16.7	-5 53 45	15.9	17.39	17.26	1
26							
27	MG 0509+0541	5 9 25.9	+5 41 35	16	15.62	15.18	0.60
28	HS 0624+6907	6 30 2.4	+69 5 4	14.4	14.43	14.09	0.49
29	1ES 0647+250	6 50 46.5	+25 3 0	15.3	15.84	15.45	0.92
30	MS 07007+6338	7 5 29.4	+63 33 33	15.7	15.58	15.33	0.26
31	7ZW 118	7 7 13.2	+64 35 59	14.6	15.37	14.92	0.58
32	B2 0709+370	7 13 9.4	+36 56 7	15.5	15.70	15.48	0.72
33	4C 41.30	7 45 41.6	+31 42 56	15.6	15.68	15.54	0.72
34	OI+90.4	7 57 6.7	+9 56 35	15	17.21	16.57	0.37
35	NAME DISPUTE	7 58 0.1	+39 20 30	14.4			
36	IRAS 07598+6508	8 4 30.4	+64 59 53	15.5	14.67	14.45	0.62

Number	Object	R.A.	Dec	VC MAG	Measured V	Measured R	R^2
37	MS 08019+2129	8 4 53	+21 20 41	15.9			
38	1ES 0806+524	8 9 49.2	+52 18 58	15.3	15.34	14.90	0.93
39	PG 0804+761	8 11 32.7	+76 1 54	14.7	14.69	14.46	0.98
40	PG 0832+251	8 35 35.9	+24 59 41	15.9	16.49	16.10	0.73
41	US 1329	8 36 58.9	+44 26 2	15.6	15.58	15.30	0.38
42	CSO 199	8 41 18	+35 44 38	16	16.81	16.51	0.07
43	7ZW 244	8 44 45.3	+76 53 10	15.7	16.26	15.94	0.18
44	0846+51W1	8 49 58	+51 8 29	15.7			
45	SBS 0909+532	9 13 2.5	+52 59 37	16	16.52	15.90	0.82
46	TON 1057	9 25 54.7	+19 54 4	15.8	15.39	15.06	0.95
47	MK 707	9 37 1.1	+1 5 43	16			
48	TON 1078	9 37 1.9	+34 25 0	16	16.37	16.13	0.78
49	4C 12.35	9 45 49.9	+12 5 31	16	18.69	18.53	1
50	K 348-7	9 56 52.3	+41 15 21	15.3			
51	3C 232	9 58 20.9	+32 24 2	15.8	15.82	15.52	0.34
52	MK 132	10 1 29.7	+54 54 38	16	16.23	15.93	0.93
53	FBS 787	10 3 6.7	+68 13 18	15.9			
54	4C 13.41	10 7 26.2	+12 48 56	15.2	15.61	15.25	1

Number	Object	R.A.	Dec	VC MAG	Measured V	Measured R	R^2
55	TON 488	10 10 0.7	+30 3 21	16	17.013	16.63	0.28
56	CSO 38	10 11 55.7	+29 41 41	16			
57	TON 1187	10 13 3.1	+35 51 22	15.4	15.98	15.55	0.78
58	SBS 1010+535	10 13 26.6	+53 16 8	16	16.44	16.15	0.38
59	PG1011-040	10 14 20.7	-4 18 39	15.5			
60	PG1012+008	10 14 54.9	+0 33 37	15.6			
61	TON 34	10 19 56.6	+27 44 2	15.7	16.39	16.01	1
62	B3 1019+397	10 22 37.5	+39 31 51	16	17.11	16.79	0.71
63	MK 142	10 25 31.3	+51 40 35	16	15.70	15.22	1
64	SBS 1047+550	10 50 45.7	+54 47 20	16	16.93	16.85	0.45
65	RX J10547+4831	10 54 44.6	+48 3 39	15.7	16.59	16.35	0.29
66	TON 52	11 4 7	+31 41 11	16	16.63	16.39	1
67	3C 249.1	11 4 13.8	+76 58 58	15.7	15.52	15.21	0.54
68	MK 421	11 4 27.2	+38 12 32	12.9	13.14	12.71	0.97
69	HS 1103+6416	11 6 10.8	+64 0 8	15.8	15.87	15.43	1
70	4C 16.30	11 7 15.1	+16 28 3	15.7	16.75	17.00	1
71	TON 1388	11 19 8.8	+21 19 18	14.7	15.01	14.76	1
72	SBSG 1116+518	11 19 43.1	+51 33 35	15	17.36	17.08	0.42

Number	Object	R.A.	Dec	VC MAG	Measured V	Measured R	R^2
73							
74	S4 1128+38	11 30 53.4	+38 15 20	16	19.34	18.55	
75	TON 580	11 31 9.4	+31 14 7	16	16.67	16.36	1
76	MK 180	11 36 26.5	+70 9 28	14.5	14.68	14.14	0.79
77	WAS 26	11 41 16.1	+21 56 22	14.9	15.39	15.13	
78	RX J11479+2715	11 47 54.4	+27 15 0	15.4	16.42	16.11	1
79	CBS 147	11 50 9.5	+34 56 31	16	17.93	17.51	0.57
80	OM+280	11 50 19.2	+24 17 54	15.7	16.70	16.18	1
81	PG 1151+118	11 53 49.3	+11 28 30	16	16.30	16.01	1
82	TON 599	11 59 31.9	+29 14 45	14.4	17.03	16.63	0.9
83	GQ Com	12 4 42 1	+27 54 12	15.6	16.66	16.25	1
84	PG 1206+459	12 8 58	+45 40 36	15.7	15.58	15.35	1
85	PG 1211+143	12 14 17.7	+14 3 13	14.2	14.78	14.56	1
86	1ES 1212+078	10 15 11	+7 32 4	16	16.85	16.12	1
87	ON+325	12 17 52	+30 7 1	15.6	14.90	14.48	1
88							
89	PG 1216+069	12 19 20.9	+6 38 38	15.7			
90	RS4	12 21 21.9	+30 10 37	15.9			

Number	Object	R.A.	Dec	VC MAG	Measured V	Measured R	R^2
91	MK 205	12 21 44.1	+75 18 38	15.2	15.53	14.86	0.7
92	TON 618	12 28 24.8	+31 28 38	15.9	15.99	15.68	1
93	3C 273.0	12 29 6.7	+2 3 8	12.9	13.12	12.91	1
94	RX J12302+2517	12 30 14	+25 18 7	15.6	16.19	16.04	0.96
95	TON 1542	12 32 3.6	+20 9 30	15.3	15.07	14.6	1
96	TON 83	12 33 41.7	+31 1 2	16	16.77	16.48	1
97	CSO 151	12 33 55.4	+29 7 48	16	17.13	16.63	0.80
98	SBS 1234+607	12 36 22.1	+60 30 21	16	18.37	17.86	1
99	PG 1241+176	12 44 10.8	+17 21 4	15.9	16.33	15.94	1
100	PG 1246+586	12 48 18.8	+58 20 29	15.5	16.33	15.92	0.94
101	LB 19	12 50 5.7	+26 31 7	15.6	15.71	15.37	1
102	KUV 12491+2932	12 51 28.8	+29 15 26	15.5	16.23	15.96	1
103	Q 1252+0200	12 55 19.7	+1 44 13	15.5	16.29	16.03	0.98
104	1ES 1255+244	12 57 31.9	+24 12 40	15.4	17.29	16.73	1
105	LB 2522	13 1 12.9	+59 2 7	15.8	15.72	15.28	1
106							
107	PG1307+086	13 9 47	+8 19 49	15.1	16.09	15.76	0.90
108	OP+313	13 10 28.7	+32 20 44	15.2	18.56	18.57	1

Number	Object	R.A.	Dec	VC MAG	Measured V	Measured R	R^2
109	TON 1565	13 12 17.7	+35 15 23	15.6	15.53	15.24	1
110	TON 153	13 19 56	+27 28 10	16	15.97	15.77	0.48
111	PG 1322+059	13 23 49.6	+65 41 48	15.8	15.66	15.42	1
112	Q 1326-0516	13 29 28.6	-5 31 36	15.6			
113	4C 55.27	13 34 11.6	+55 1 25	16	18.20	18.02	1
114	TON 730	13 43 56.6	+25 38 52	15.9	15.95	16.59	0.48
115							
116	CSO 1022	13 53 26	+36 20 49	16	16.52	16.18	1
117	MK 662	13 54 6.4	+23 25 49	15.4	15.51	15.08	0.99
118	PB 4142	13 54 35.6	+18 5 18	15.9	16.36	15.99	1
119							
120	TON 182	14 5 16.2	+25 55 34	15.5	16.10	15.81	0.54
121	PG 1404+226	14 6 21.9	+22 23 47	15.8	15.98	15.67	1
122							
123	PG 1411+442	14 9 23.9	+26 18 21	15.7	14.94	14.63	1
124	PG 1411+442	14 13 58.9	+43 58 59	15			
125	PG 1415+451	14 17 0.8	+44 56 6	15.7	15.91	15.51	1
126	1E 1415+259	14 17 56.6	+25 43 25	16	17.08	16.53	1

Number	Object	R.A.	Dec	VC MAG	Measured V	Measured R	R^2
127	OQ+530	14 19 46.6	+54 23 14	15.7	15.67	15.13	0.86
128	KUV 14207+2308	14 22 57.7	+22 54 41	15.6	16.01	15.65	1
129	2E 1423+2008	14 26 13.4	+19 55 25	16	16.84	16.39	1
130	PKS 1424+240	14 27 0.5	+23 48 0	15	14.76	14.36	0.96
131	MK 813	14 27 25	+19 49 52	15.3	14.98	14.70	1
132	TON 202	14 27 35.7	+26 32 14	15.7	16.83	16.56	1
133	MK 1383	14 29 6.6	+1 17 6	14.9	14.54	14.21	1
134							
135	PG 1437+398	14 39 17.5	+39 32 44	16	16.94	16.42	0.81
136	MARK 478	14 42 18.6	+35 25 14	14.6	14.71	14.36	1
137	PG 1444+407	14 46 46	+40 35 6	15.7	16.07	0.5315.75	
138	3C 305.0	14 49 27.4	+63 15 7	13.7	14.17	13.57	1
139	MK 830	14 50 26.6	+58 39 45	16	17.31	16.78	0.57
140	MK 840	15 4 8.5	+14 31 26	16	16.51	15.90	0.96
141	1H 1515+660	15 17 47.5	+65 25 23	15.9	17.09	16.82	0.84
142	MCG 11.19.006	15 19 25.3	+65 33 42	13.9	15.73	15.09	0.99
143							
144							

Number	Object	R.A.	Dec	VC MAG	Measured V	Measured R	R^2
145	RX J15291+5616	15 29 7.4	+56 16 7	15.8	16.59	16.35	0.29
146	PG 1538+478	15 39 34.8	+47 35 31	15.8	16.05	15.83	0.52
147	1ES 1544+820	15 40 15.8	+81 55 7	15.3	17.30	16.75	0.45
148	SBS 1542+542	15 43 59.3	+53 59 3	16	17.28	17.03	1
149	MK 876	16 13 57.2	+65 43 9	15.5	14.85	14.49	0.97
150	TON 256	16 14 13.2	+26 4 16	15.4	15.99	15.61	0.32
151	3C 332.0	16 17 42.7	+32 22 34	16	15.88	15.38	0.91
152	MK 877	16 20 11.3	+17 24 28	15.4	15.33	15.09	0.70
153	KP 77	16 25 48.8	+26 46 59	16	17.33	17.13	0.90
154	HS 1626+6433	16 26 45.7	+64 26 54	15.8	16.66	16.34	0.36
155	KUV 16313+3931	16 33 2.2	+39 24 27	16	16.69	16.39	0.22
156	3C 345.0	16 42 58.8	+39 48 37	16	18.71	18.04	0.30
157	MK 501						
158	RX J17025+3247	17 2 31	+32 47 17	15.9	16.20	15.90	0.40
159	3C 351.0	17 4 41.5	+60 44 28	15.3	15.67	15.23	0.89
160	RX J17159+3112	17 16 2.1	+31 12 13	16	15.81	15.46	0.86
161	PG 1718+481	17 19 38.4	+48 4 13	14.6	15.10	14.66	0.34
162	4C 34.47	17 23 20.8	+34 17 59	15.5	16.32	15.91	0.91

Number	Object	R.A.	Dec	VC MAG	Measured V	Measured R	R^2
163	H 1722+119	17 25 4.4	+11 52 16	15.8	15.52	14.85	0.38
164	1ZW 187	17 28 18.6	+50 13 11	16	15.90	15.37	0.41
165	IRAS 17371+5615	17 38 1.6	+56 13 25	15.2	16.28	15.59	0.24
166	IRAS 17490+2659	17 51 5.5	+26 59 2	15.1			
167	IRAS 17500+5046	17 51 16.7	+50 45 37	15.4	15.24	14.83	0.57
168	KAZ 102	18 3 28.9	+67 38 10	15.8	16.57	16.24	0.69
169	KUV 18217+6419	18 21 58.7	+64 20 45	14.2	14.23	13.87	0.74
170	PGC 61965	18 30 23.3	+73 13 10	15.5	15.09	14.69	0.72
171	IRAS 18299+4113	18 31 34.5	+41 16 5	15.4	16.22	15.73	0.10
172	HS 1946+7658	19 44 45.2	+77 6 32	15.8	16.42	16.05	0.37
173	1ES 1959+650	19 59 59.9	+65 8 55	12.8	14.95	14.39	0.89
174	4C 74.26	20 42 37.3	+75 8 2	15.1	14.69	14.14	0.25
175	MK 509	20 44 9.7	-10 43 24	13.1	13.79	13.25	0.86
176	PG 2112+059	21 14 52.6	+6 7 42	15.8	15.62	15.317	0.78
177	2ZW 136	21 32 27.8	+10 8 19	14.6	14.77	14.41	0.78
178	OX+169	21 43 35.5	+17 43 49	15.7	16.18	15.82	0.16
179	IRAS 21431-0432	21 45 45.8	-4 18 4	15.7	16.54	16.05	0.19
180	BL Lac	22 2 43.3	+42 16 39	14.7	14.12	13.39	0.21

Number	Object	R.A.	Dec	VC MAG	Measured V	Measured R	R^2
181	4C 31.63	22 3 14.9	+31 45 38	15.6	15.61	15.21	0.49
182	2ZW 171	22 11 53.9	+18 41 49	15.4			
183	KUV 22497+1439	22 52 8	+14 54 49	15.9	16.11	15.75	0.25
184	4C 11.72	22 54 10.5	+11 36 38	15.8	15.86	15.41	0.13
185	MK 926	23 4 43.5	-8 41 8	13.8	14.66	14.07	0.79
186	PB 5235	23 4 45	+3 11 46	15.8	15.95	15.69	0.80
187	PB 5250	23 7 3	+4 32 57	15.5	15.40	14.71	0.80
188	4C 09.72	23 11 17.7	+10 8 15	16	16.15	16.00	0.86
189	3C 465.0	23 38 43	+27 3 22	13.3	13.67	12.96	0.01
190	4C 09.74	23 46 37	+9 30 45	16	16.28	16.07	0.08
191	1ES 2344+514	23 47 4.8	+51 42 18	15.5	15.38	14.62	
192	PKS 2349-014	23 51 56.1	-1 9 13	15.3	16.37	15.80	

Table 3.1 VC MAG: Measured V magnitude at the time of discovery as given in Veron Cetty; Measured V& R: Averaged magnitudes through ROVOR's observations; R^2: Correlation coefficient found with our data. Missing data indicates data which was unable to be reduced reasonably

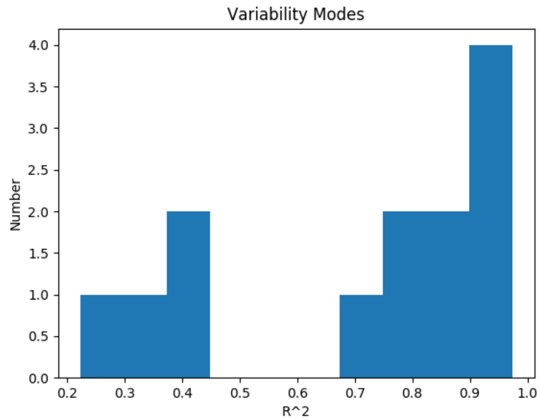

Figure 3.2 Blazar variability clusters.

Our data seems to fit comfortably into two categories: smooth or stochastic. This indicates two kinds of flaring mechanism as predicted. As we have stated, there is a possibility that each object behaves as a combination of these patterns; data needs to be taken over a longer period of time before this can be determined.

The R^2 values of the 13 objects with significant deviation ratios are shown in figure 3.2. Two groups can be seen. The group on the left is stochastic, and the right is smooth.

3.2 Conclusions

Overall we found four percent of our objects to flare over the observational period of a year. Assuming this rate can be generalized over the entire population, this correlates to an average flaring rate of once every 15 years. Obviously more data needs to be taken before we can know if this number can be generalized or not.

This frequency is much lower than expected considering one of the primary characteristics of blazars is their almost continuous flaring behaviour. Therefore we can conclude that either many objects go dormant, or the categorization of many these objects needs to be reassessed.

Additionally it is possible that a lower flaring frequency is a characteristic of brighter blazars, and the assumed characteristic of higher frequency flaring is only found in the dimmer populations that have previously been thoroughly observed.

Bibliography

Moody, J. W., Boizelle, B., Bates, K., Little, B., McCombs, T., Nelson, J.,Pace, C., Pearson, R. L. III, Harrison, J., Brown, P.J., and Barnes, J., PASP, 124, 956-962, 2012 (arXiv:astro-ph/0590641)

Veron-Cetty M.P., Veron P., Astron. Astrophys. 518, A10, 2010; https://heasarc.gsfc.nasa.gov/W3Browse/all/veroncat.html

Smith, Alex G., Nair, A. D., PASP, 107, 863-870, 1995; http://iopscience.iop.org/article/10.1086/133634/pdf